HHS Public Access

Author manuscript

Clin Cancer Res. Author manuscript; available in PMC 2019 November 05.

Published in final edited form as:

Clin Cancer Res. 2018 November 15; 24(22): 5585–5593. doi:10.1158/1078-0432.CCR-18-0937.

SPOP-Mutated/CHD1-Deleted Lethal Prostate Cancer and Abiraterone Sensitivity

Gunther Boysen[#1], **Daniel N. Rodrigues**[#1], **Pasquale Rescigno**[2], **George Seed**[1], **David Dolling**[1], **Ruth Riisnaes**[1], **Mateus Crespo**[1], **Zafeiris Zafeiriou**[2], **Semini Sumanasuriya**[2], **Diletta Bianchini**[2], **Joanne Hunt**[2], **Deirdre Moloney**[2], **Raquel Perez-Lopez**[3], **Nina Tunariu**[2], **Susana Miranda**[1], **Inês Figueiredo**[1], **Ana Ferreira**[1], **Rossitza Christova**[1], **Veronica Gil**[1], **Sara Aziz**[1], **Claudia Bertan**[1], **Flavia M. de Oliveira**[1], **Mark Atkin**[1], **Matthew Clarke**[1], **Jane Goodall**[1], **Adam Sharp**[1], **Theresa MacDonald**[4,5], **Mark A. Rubin**[4,5,6], **Wei Yuan**[1], **Christopher E. Barbieri**[4,7], **Suzanne Carreira**[1], **Joaquin Mateo**[3], **Johann S. de Bono**[1,2]

[1]Institute of Cancer Research, London, United Kingdom. [2]Prostate Cancer Targeted Therapy Group and Drug Development Unit, The Royal Marsden NHS Foundation Trust, London, United Kingdom. [3]Vall D'Hebron Institute of Oncology, Barcelona, Spain. [4]Sandra and Edward Meyer Cancer Center, Weill Cornell Medicine, New York, New York. [5]Englander Institute for Precision Medicine, Weill Cornell Medicine, New York-Presbyterian Hospital, New York, New York. [6]Department of Biomedical Research, University of Bern, Bern, Switzerland. [7]Department of Urology, Weill Cornell Medicine, New York-Presbyterian Hospital, New York, New York.

[#] These authors contributed equally to this work.

Abstract

Corresponding Author: Johann S. de Bono, The Institute of Cancer Research and The Royal Marsden NHS Foundation Trust, London SM2 5NG, United Kingdom. Phone: 4420-8722-4028; Fax: 4420-8642-7979; johann.de-bono@icr.ac.uk.

Authors' Contributions

Conception and design: G. Boysen, D.N. Rodrigues, M.A. Rubin, W. Yuan, C.E. Barbieri, J. Mateo, J.S. de Bono

Development of methodology: G. Boysen, D.N. Rodrigues, R. Riisnaes, I. Figueiredo, J.S. de Bono

Acquisition of data (provided animals, acquired and managed patients, provided facilities, etc.): G. Boysen, D.N. Rodrigues, P. Rescigno, R. Riisnaes, M. Crespo, S. Sumanasuriya, D. Bianchini, J. Hunt, D. Moloney, R. Perez-Lopez, N. Tunariu, S. Miranda, A. Ferreira, R. Christova, V. Gil, C.Bertan, F.M. de Oliveira, M. Atkin, J. Goodall, A. Sharp, T. MacDonald, S. Carreira, J. Mateo, J. S. de Bono

Analysis and interpretation of data (e.g., statistical analysis, biostatistics, computational analysis): G. Boysen, D.N. Rodrigues, P. Rescigno, G. Seed, D. Dolling, R. Christova, C.E. Barbieri, S. Carreira, J. Mateo, J.S. de Bono

Writing, review, and/or revision of the manuscript: G. Boysen, D.N. Rodrigues, P. Rescigno, R. Riisnaes, Z. Zafeiriou, S. Sumanasuriya, R. Perez-Lopez, N. Tunariu, S. Miranda, I. Figueiredo, A. Ferreira, J. Goodall, A. Sharp, W. Yuan, C.E. Barbieri, S. Carreira, J. Mateo, J.S. de Bono

Administrative, technical, or material support (i.e., reporting or organizing data, constructing databases): G. Boysen, P. Rescigno, S. Aziz, F.M. de Oliveira, M. Clarke, W. Yuan J.S. de Bono

Study supervision: G. Boysen, W. Yuan, C.E. Barbieri, J.S. de Bono

Disclosure of Potential Conflicts of Interest

G. Boysen is an employee of and has ownership interests (including patents) at Astellas Pharma UK. D. Bianchini reports receiving speakers bureau honoraria from Janssen. M.A. Rubin is a coinventor on a pending patent application for SPOP mutations and associated copy-number alterations. J. Mateo reports receiving speakers bureau honoraria from Astellas and Sanofi. J.S. de Bono is a consultant/advisory board member for Astellas Pharma, AstraZeneca, Bayer, Genmab, Genentech, GlaxoSmithKline, Janssen, Medivation, Orion Pharma, Pfizer, and Sanofi. No potential conflicts of interest were disclosed by the other authors.

The costs of publication of this article were defrayed in part by the payment of page charges. This article must therefore be hereby marked *advertisement* in accordance with 18 U.S.C. Section 1734 solely to indicate this fact.

Note: Supplementary data for this article are available at Clinical Cancer Research Online (http://clincancerres.aacrjournals.org/).

Purpose—*CHD1* deletions and *SPOP* mutations frequently cooccur in prostate cancer with lower frequencies reported in castration-resistant prostate cancer (CRPC). We monitored CHD1 expression during disease progression and assessed the molecular and clinical characteristics of *CHD1* -deleted/*SPOP*-mutated metastatic CRPC (mCRPC).

Experimental Design—We identified 89 patients with mCRPC who had hormone-naive and castration-resistant tumor samples available: These were analyzed for CHD1, PTEN, and ERG expression by IHC. *SPOP* status was determined by targeted next-generation sequencing (NGS). We studied the correlations between these biomarkers and (i) overall survival from diagnosis; (ii) overall survival from CRPC; (iii) duration of abiraterone treatment; and (iv) response to abiraterone. Relationship with outcome was analyzed using Cox regression and log-rank analyses.

Results—CHD1 protein loss was detected in 11 (15%) and 13 (17%) of hormone-sensitive prostate cancer (HSPC) and CRPC biopsies, respectively. Comparison of CHD1 expression was feasible in 56 matched, same patient HSPC and CRPC biopsies. CHD1 protein status in HSPC and CRPC correlated in 55 of 56 cases (98%). We identified 22 patients with somatic *SPOP* mutations, with six of these mutations not reported previously in prostate cancer. *SPOP* mutations and/or CHD1 loss was associated with a higher response rate to abiraterone (SPOP: OR, 14.50 $P = 0.001$; CHD1: OR, 7.30, $P = 0.08$) and a longer time on abiraterone (SPOP: HR, 0.37, $P = 0.002$, CHD1: HR, 0.50, $P = 0.06$).

Conclusions—*SPOP*-mutated mCRPCs are strongly enriched for CHD1 loss. These tumors appear highly sensitive to abiraterone treatment.

Introduction

Adenocarcinomas of the prostate comprise a heterogeneous collection of malignancies with distinct molecular underpinnings. Linking molecular background to clinical outcome, that is, tumor progression and response to therapy, remains an unmet need in prostate cancers. So far, genomic alterations are still not validated as molecular markers for patient stratification for current standard treatments in this disease. This is partially due to the lack of well-annotated patient cohorts, which cover disease evolution from localized, hormone-naïve disease to metastatic castration-resistant prostate cancer (mCRPC).

Deletions in the gene encoding the chromodomain helicase DNA-binding protein 1 (CHD1) and mutations in the gene encoding the Speckle-Type POZ protein (SPOP) are among the most frequent genomic alterations in prostate cancer (up to 29%; refs. 1–6). CHD1 is an ATPase-dependent helicase mediating a variety of biological processes including maintenance of open chromatin, DNA damage repair, and transcription (7). SPOP is part of an E3-ubiquitin ligase complex that is involved in controlling protein stability of the androgen receptor (AR) and some of its transcriptional coactivators (8–10). In prostate cancer, mutations specifically impact the MATH protein domain of SPOP, leading to increased stability of its substrates and deregulation of diverse molecular pathways impacting transcription, invasion, genome instability, and drug resistance (2, 10–14). Loss of *CHD1* significantly cooccurs with mutations in *SPOP* (2, 4, 5). Patients bearing these genomic alterations form a molecular subclass of prostate cancer with increased AR transcriptional activity, absence of *ERG* rearrangements, and specific epigenetic pattern (4).

Importantly, a recent study of multiparametric MRI (mpMRI) in localized prostate cancer suggests that *CHD1* -deleted foci may associate with a less aggressive imaging phenotype (15). Whether and how *CHD1* loss and *SPOP* mutation impact progression to lethal metastatic disease is, however, still unclear. Recent next-generation DNA sequencing studies suggest significantly different *CHD1* deletion and *SPOP* mutation frequencies when comparing localized prostate cancer with mCRPC (4, 5). This either suggests better outcome for these tumors to initial therapy or a more indolent clinical behavior. However, these observations are difficult to interpret because disease molecular evolution during progression has not been monitored.

Genomic sequencing studies have enabled the molecular stratification of prostate cancer, identifying diverse subclasses with the promise of developing novel therapeutic strategies to deliver more precise patient care and improving outcome. Abiraterone improves survival in men with mCRPC, but the benefit derived varies substantially between patients (16). Limited information is available for improving patient selection for such therapies. Because *CHD1* deletions and *SPOP* mutations reflect a common molecular prostate cancer subclass with increased AR activity, we evaluated the clinical outcome from these cancers hypothesizing that these tumors would be highly sensitive to abiraterone treatment.

Materials and Methods

Patient selection, clinical data, and study design

Biopsies from bone, lymph node, and liver metastases were obtained from patients with mCRPC treated at the Royal Marsden Hospital (London, United Kingdom) between 2010 and 2016 and that were (i) fit enough to participate in a clinical trial and (ii) consented for next-generation DNA sequencing analysis. All patients gave their written informed consent and were enrolled on institutional protocols approved by the Royal Marsden NHS Foundation Trust Hospital Ethics Review Committee (reference No. 04/Q0801/60). CRPC biopsies were acquired between 2010 and 2016 in accordance with the ethical guidelines of the Helsinki Declaration. Clinical data including response to treatment were retrospectively collected from electronic patient records. Patients received abiraterone treatment in UK centers between November 2006 and December 2015. Response to therapy was defined on the basis of RECIST version 1.1 criteria and/or PSA falls ≥50% from baseline (17). This study was designed as a case-control study with SPOP-mutant patients being selected on the basis of DNA sequencing data and being matched with unselected SPOP wild-type patients as controls.

Cell lines

22Rv1 (ATCCCRL-2505), PC-3 (ATCCCRL-1435), and NCI-H660 (ATCCCRL-5813) prostate cancer cell lines were purchased from ATCC and cultured according to the manufacturer’s protocol. CHD1 CRISPR clones were derived as described earlier (7).

siRNA transfection

siRNAs targeting CHD1 and nontargeting controls were purchased from Dharmacon (siGENOME SMARTpool CHD1: M-008529–01-0005, siGENOME SMARTpool

nontargeting control: D-001206–13-05). siRNA oligonucleotides were transfected with lipofectamine 3000 (Life Technologies) at a final concentration of 100 pmol and incubated for 48 hours.

Immunoblotting

22Rv1 isogenic CRISPR clones, siRNA transfected 22Rv1, PC-3, and NCI-H660 cells were harvested in RIPA buffer (Pierce, 89900) containing protease and phosphatase inhibitors (complete mini protease inhibitor cocktail tablets, Roche, 11374600). The soluble fraction was isolated using centrifugation and quantified by bicinchoninic acid assays (BCA; Pierce, QG219588). Cell lysates were mixed with LDS sample buffer (Life Technologies, 1621149) and 30 to50 mg of total protein was loaded onto 4% to12% gradient SDS acrylamide gels (Life Technologies, NP0322). Transfer to PDVF membrane (Millipore, IPV400010) was performed at 90 V for 90 minutes at room temperature. Protein bands were detected using HRP-substrate (Millipore, WBLUC0500). Primary antibodies were anti-CHD1 rabbit mAb (clone D8C2, Cell Signaling Technology, 4351) and anti-GAPDH (clone 6C5, Millipore, MAB374). Secondary antibodies were anti-rabbit and anti-mouse horseradish peroxidase-conjugated whole antibody from sheep (GE, NA934V, and NXA93).

IHC

IHC was performed on 3 μmol/L formalin-fixed and paraffin-embedded (FFPE) tissue sections. Heat-based antigen retrieval was performed by boiling the tissue sections in pH6 citrate buffer (TCS Biosciences Ltd., HDS05, 1:100 dilution) for 18 minutes using a microwave. CHD1 immunostaining was done on the Launch i6000 IHC autostainer using a 1:50 dilution of primary antibody-binding CHD1 (Cell Signaling Technology, #4351) for 1 hour. Visualization of antibody binding was achieved using the Novolink polymer detection method (Leica, RE7200-CE). To avoid false negative results, we defined endothelial cell CHD1 expression as a necessary internal control for samples to be included in the analysis. IHC for PTEN and ERG was done as reported previously (18, 19). Tumor content, morphology, and intensity of protein expression were evaluated by a pathologist (D.N. Rodrigues). H-score was defined as described earlier (18). The cutoff for CHD1 protein loss was defined as H-score ≤5.

FISH

FISH for assessing *CHD1* copy-number status in FFPE tumor tissue was performed as described previously (18). The probes were *CHD1* (RP11–58M12, chr. 5q21) and reference (RP11–429D13, chr. 5p13.1). Probes were amplified using the GenomiPhi v3 DNA amplification Kit (Illustra, 25–6601-24) and directly labeled with CY3 (CHD1) and CY5 using the Bioprime DNA labeling system (Thermo Fisher Scientific, 18094011). Fluorescence images were taken using the BioView Duet imaging system and copy-number status of at least 50 nonoverlapping tumor cell nuclei was determined by a pathologist (D.N. Rodrigues).

DNA sequencing

DNA isolation—DNA from tumor tissue biopsies was extracted using the QIAamp DNA FFPE Tissue Kit (Qiagen), quantified by Quant-iT Picogreen double-stranded DNA (dsDNA) Assay Kits (Invitrogen, Thermo Fisher Scientific). The Illumina FFPE QC Kit (WG-321–1001) was used for DNA quality control tests.

Targeted sequencing—Libraries were prepared using a customized GeneRead v2 DNAseq Panel (Qiagen) consisting of 113 genes including *SPOP* as described previously (20, 21). Libraries were read on the Illumina MiSeq platform.

Sequence alignment—FASTQ files were generated using the Illumina MiSeq Reporter v2.5.1.3. Sequence alignment and mutation calling were performed using BWA tools and the GATK variant annotator by the Qiagen GeneRead Targeted Exon Enrichment Panel Data Analysis Web Portal.

Bioinformatic analysis

Mutation burden—The mutation burden was estimated from targeted next-generation sequencing (NGS) panel data after filtering out of spurious and germline variants using methods reported previously (22). Genetic variants were called using the GATK pipeline (23). Low-quality variants were removed (haplotype score > 200, mapping quality <40, coverage depth <60, alternative allele < 5% of reads, multiallelic calls, indels, known poorly sequenced sites). Variants were then annotated using Oncotator (version 1.8.0; ref. 24). Germline variants were defined when the allele frequency was > 5% in our cohort or in two or more public databases (ExAC; ref. 25), 1000 Genomes (The 1000 Genomes Project Consortium; ref. 26) and dbSNP (27), or with more than 99.9% of the reads being the alternate allele. These germline variants were filtered out. Finally, point mutations described as somatic in the COSMIC database (28) at least 10 times or more were then “added” back into the mutation count.

Copy-number burden—Following the assessment of copy-number variation from targeted NGS, we calculated copy-number burden as the proportion of evaluable genes (n = 99) bearing any detectable change, that is, a $\log_2$ ratio of greater or less than 0.4 and −0.4, respectively (21). Samples were included in the analysis if the total read count was > 500 K, > 95% of properly paired reads, > 99.9% reads on target, and IQR > 0.8.

Shannon index—Given counts of FISH probes for a minimum of 50 individual cells on a per-sample basis, we calculated intercellular diversity by classifying each cell by the state of both probes, totaling the number of each class, and applying the R package Vegan (v.2.4.4) to generate the Shannon–Weaver diversity index H.

Statistical analysis

Clinical characteristics at diagnosis (age, Gleason score, and metastatic disease), and treatments received, were compared by CHD1 status at CRPC using Wilcoxon rank-sum tests or Fisher exact test if categorical. Baseline levels of PSA, hemoglobin, alkaline phosphatase, lactate dehydrogenase, and albumin at the start of abiraterone treatment were

compared by CHD1 and *SPOP* status at CRPC using *t* tests or Wilcoxon rank-sum tests if considered to be nonnormally distributed. Data on castration resistance were determined retrospectively from patient's medical records. The change in CHD1 H-score in patient-matched hormone-sensitive prostate cancer (HSPC) and CRPC samples was compared using the Wilcoxon matched-pairs signed-rank test. Overall survival (OS) from diagnosis, CRPC, and the start of abiraterone treatment was compared by CHD1 and SPOP status using Kaplan–Meier plots. Univariate Cox models were used to evaluate the association of metastatic disease at diagnosis, *SPOP* mutation, CHD1 negativity, and ERG expression at CRPC with OS from diagnosis, time on abiraterone, and time from start of LHRH to CRPC. Univariate logistic regression analyses also evaluated the association of these characteristics with response to abiraterone, defined as radiographic response according to the RECIST 1.1, and/or a ≥50% fall in PSA from baseline (17). All analyses were conducted using Stata v13.1.

Results

Establishing a CHD1 IHC assay

To determine the frequency of CHD1 protein loss across a spectrum of clinical states, we established and validated an IHC-based assay for FFPE tissue. We first evaluated FFPE human prostate cancer cell lines that either had an amplification (PC-3) or deletion (NCI-H660) of *CHD1* confirmed by FISH (Fig. 1A). To further ensure the specificity of the antibody, we depleted CHD1 in the CRPC cell line 22Rv1 transiently by siRNA as well as stably by CRISPR/CAS9. Western blot analysis using the same CHD1 antibody revealed a major decrease of CHD1 protein after siRNA and CRISPR/CAS9 treatment (Fig. 1B). The loss of CHD1 after CRISPR/CAS9 knockout in this isogenic model was further validated in FFPE cells (Fig. 1B). Finally, we implemented the IHC assay in human tumor biopsies from 44 patients with prostate cancer (12 HSPC, 32 CRPC) representative of the most common sites of disease (13 bone, nine lymph node, five liver, three soft tissue, and two TURP biopsies) and compared CHD1 expression with gene copy number determined by FISH. Overall, three of 44 (7%) had loss of both CHD1 expression by IHC as well as gene loss by FISH. CHD1 protein expression by IHC and gene copy-number status by FISH was strongly associated (Fig. 1C and D).

Molecular features of CHD1-deleted CRPC

To explore the molecular features of *CHD1* -deleted lethal prostate cancer, we selected 89 patients for whom we had CRPC biopsies (Supplementary Fig. S1A) enriching this cohort for *CHD1* loss CRPC by including tumors with known *SPOP* mutations based on data from prior molecular characterization studies. We performed IHC for CHD1 in paired, same patient, CRPC and HSPC biopsies from these 89 subjects. The IHC data were analyzable for 73 (82%) and 83 (93%) HSPC and CRPC biopsies, respectively. We identified 11 (15.1%) and 13 (16.9%) HSPC and CRPC biopsies, respectively, with complete loss of CHD1 protein (Fig. 2A). Targeted or whole-exome DNA sequencing data were available for 71 (79.7%) patients (CRPC biopsies: $n = 69$, HSPC biopsies: $n = 2$), with 22 of these carrying a mutation that affects SPOP (Fig. 2B). We identified six mutations that have not been described previously in prostate cancer before, including one (p.A187T) located in the BTB

domain in an area reported to be necessary for homodimerization (Fig. 2B; Supplementary Table S1): two of these six mutations were located in residues (E50, R121) previously associated with endometrial cancer (29). The overall distribution of altered residues was, however, similar to other CRPC cohorts resulting in two distinct mutational hotspots in the MATH domain (Supplementary Fig. S2B). Loss of CHD1 and/or *SPOP* mutation ($CHD1^{Loss}/SPOP^{MUT}$) was found in a total of 22 patients (24.7%). All CHD1 loss cases that could be analyzed by targeted sequencing (11/13 could be sequenced), had an *SPOP* mutation ($P < 0.0001$; Table 1; Fig. 2A). We performed ERG IHC analysis in our CRPC cohort and confirmed a mutually exclusive relationship between *SPOP* mutations and CHD1 loss and ERG overexpression ($P < 0.001$ for SPOP; $P = 0.003$ for CHD1; Fig. 2A). Prior genomic studies in localized prostate cancer have suggested a synthetic lethal relationship between *CHD1* loss and loss of the tumor suppressor *PTEN.* Surprisingly, our analysis identified two cases (2.4%) of combined CHD1 and PTEN protein loss, suggesting that although the majority of $CHD1^{Loss}/SPOP^{MUT}$ tumors in our cohort do not have PTEN loss, certain genomic backgrounds tolerate the concurrent loss of these two proteins (Fig. 2A; Supplementary Fig. S2A). To investigate the impact of *SPOP* mutations on genome stability in CRPC, we estimated mutation (SNV) burden and copy-number burden on the basis of targeted NGS data from 46 analyzable CRPC samples. *SPOP* mutation did not associate with differences in SNV burden (Fig. 2C). However, *SPOP* mutation associated with increased copy-number changes ($P = 0.013$) identified by targeted NGS, similar to what we previously reported using whole-genome DNA sequencing for localized prostate cancer (Fig. 2D).

CHD1 status during disease progression

Because CHD1 loss cooccurred with *SPOP* mutations, we hypothesized that the *CHD1* gene locus is under selective pressure throughout the evolution of *SPOP*-mutant prostate cancer. To estimate the stability of the *CHD1* gene locus during tumor evolution, we evaluated copy-number states at a single-cell level using FISH in matched HSPC and CRPC biopsies. For this purpose, we determined copy-number combinations of *CHD1* (5q21) and reference probes (5p13.1) in 4,266 single cells in matched HSPC and CRPC biopsies from 36 patients and calculated the Shannon index (Fig. 2E and F). This allowed us to perform a quantitative measurement of chromosome 5 copy-number diversity at single-cell level for each biopsy. This analysis indicates that prostate cancer commonly has various degrees of intratumor genomic heterogeneity at 5p/5q with some dramatic outliers. However, *SPOP*-mutant lethal prostate cancer showed a significantly lower clonal diversity at chromosome 5 (Fig. 2F; Supplementary Fig. S2D and S2E; HSPC: $P = 0.018$, CRPC: $P = 0.0025$). When comparing the Shannon index between HSPC and CRPC patient-matched biopsies, no significant changes of genomic clonal diversity occurred with progression on androgen deprivation therapy (ADT) from HSPC to CRPC (Fig. 2F), suggesting that the loci containing *CHD1* are (i) an important driver locus in SPOP-mutant tumors and (ii) do not succumb to therapy-induced selection pressure. Thus, our analyses of patient-matched HSPC and CRPC biopsies from patients that developed lethal metastatic CRPC do not indicate a systematic depletion of *CHD1* -negative tumor clones during progression on ADT.

To evaluate whether CHD1 protein expression changes during disease progression and development of resistance to ADT, we compared patient-matched HSPC and CRPC biopsies. Overall, 56 pairs of matched, same patient, HSPC and CRPC samples were available for CHD1 expression evaluation by IHC. When categorizing our samples into CHD1 IHC negative and CHD1 IHC positive, we found that there was no change in CHD1 expression status between the matched tumor samples confirming our hypothesis that *CHD1* loss is under selective pressure during tumor progression; 55 of 56 analyzable samples (98%) maintained their CHD1 status (Fig. 2E). However, we found that overall, CHD1 expression level increases with progression from HSPC to CRPC in CHD1 IHC-positive cases ($P = 0.010$; Supplementary Fig. S2C). Tumors with CHD1 loss-of-protein expression had no detectable tumor cells expressing CHD1.

The CHD1^{Loss}/*SPOP*^{MUT} subclass and outcome from abiraterone

We investigated whether this molecular subtype of prostate cancer, defined by CHD1 loss and *SPOP* mutations (CHD1^{Loss}/*SPOP*^{MUT}) impacts clinical outcome. We evaluated the prognostic value of CHD1 loss and *SPOP* mutation and found no significant association with OS from diagnosis for either variable (Table 2). As reported previously, we also found no association between ERG expression, detecting *ERG* rearrangements, and OS (Table 2). We also analyzed the performance of known prognostic variables including presence of metastasis at diagnosis, which associated with shorter OS ($P = 0.002$). Furthermore, we did not find any association between CHD1^{Loss}/*SPOP*^{MUT} and time to resistance to ADT by LHRHa (Table 2). We found no association of CHD1^{Loss}/*SPOP*^{MUT} with OS from CRPC (Fig. 3A). However, we speculated that there might be a better response to second-line treatments such as abiraterone because preclinical data suggest a direct impact of SPOP on AR protein stability and signaling (8, 10, 12). We found that *SPOP*^{MUT} patients respond better to abiraterone when considering 50% PSA falls (SPOP: $P = 0.03$) and are less likely to progress (OR, 14.50, $P = 0.001$). Moreover, SPOP mutations are associated with longer median duration of abiraterone treatment (SPOP: HR, 0.37, $P = 0.002$). Similar trends were observed for CHD1 when considered as individual variable, although not reaching statistical significance (absence of progression: OR, 7.30, $P = 0.08$; abiraterone treatment duration: HR, 0.50, $P = 0.06$; Table 2; Fig. 3B–D; Supplementary Fig. S3A–S3C; Supplementary Table S2). In summary, our data suggest that CHD1^{Loss}/*SPOP*^{MUT} patients might respond better to abiraterone. These data need to be validated now in samples from randomized phase III clinical trials.

Discussion

Herein, we describe key molecular features of *CHD1* -deleted/*SPOP*-mutant mCRPC showing that *SPOP* mutations and CHD1 loss associate with a higher likelihood of benefit from abiraterone therapy. CHD1 loss significantly associated with *SPOP* mutations, whereas ERG rearrangements, as detected by ERG protein expression inversely correlated with CHD1 loss and *SPOP* mutation, suggesting that these genomic loci underlie selective pressure during progression to prostate cancer. We report PTEN loss largely in *CHD1* and *SPOP* wild-type backgrounds in mCRPC as reported for localized prostate cancer, but describe two patients with combined loss of CHD1 and PTEN, suggesting that a synthetic

essential relationship between these two proteins is not universal. Similar to previous reports, most of the *SPOP* mutations identified affected the SPOP-MATH domain, which is responsible for the binding of protein substrates. When comparing these mutations with other cohorts, we identified a similar distribution with two major mutational hotspots including the residues Y83-F102 and F125-F133. Surprisingly, we also identified for the first time several SPOP mutations unreported in previous systematic prostate cancer studies including E50K, S105F, Q120R, R121P, G148E, and A187T: These included two mutations affecting residues located in a less well-characterized portion of the MATH domain described previously in endometrial cancer. Whether these represent distinct functional impact unique to CRPC, or mechanistically have distinct substrate-binding specificity, will need to be elucidated in future studies.

Recent genomic studies in prostate cancer suggested a decreased frequency of *SPOP* mutations in mCRPC when compared with localized disease (8% vs. 11%; refs. 4, 5). The frequency of *CHD1* homozygous loss was reported to be 4.7% versus 9% in mCRPC versus localized disease. It has been suggested that $CHD1^{Loss}$/$SPOP^{MUT}$ tumors are generally less aggressive and that perhaps these data indicate a decreasing frequency of this subtype in mCRPC. However, our analysis in same patient, matched, treatment-naïve, and mCRPC biopsies indicate that the frequency of *CHD1* deletion does not change significantly with disease progression to mCRPC, although we cannot completely exclude subclonal differences at 5q21 at a single-cell level. Overall, our data indicate that this genotype is present from diagnosis and that there is no systematic selection generated by ADT, suggesting that the difference between the TCGA and SU2C series was most likely related to patient selection and not tumor evolution.

Despite the in-depth molecular characterization and subclassification of prostate cancer, there is currently limited understanding of how this impacts benefit from established treatments including abiraterone. A detailed understanding of the molecular characteristics of the prostate cancers sensitive or resistant to these drugs is urgently needed to help minimize overtreatment with inactive drugs. We describe here that *SPOP*-mutant and CHD1 IHC-negative mCRPC respond substantially better and longer to abiraterone when compared with mCRPC that lack these alterations. Prospective clinical trials are now needed to validate this differential response to abiraterone in this subclass of prostate cancer. Considering the early onset of these alterations in the history of prostate cancer, *SPOP* mutation/CHD1 loss may function as positive predictive biomarkers for abiraterone therapy.

This study does, however, have limitations because it is a retrospective, single-center study conducted with an intentional selection bias to enrich for *SPOP*-mutated prostate cancer. These may limit translating these results to a general unselected population of patients with prostate cancer. The impact of *SPOP*/*CHD1* status on abiraterone treatment outcome now needs prospective validation.

Supplementary Material

Refer to Web version on PubMed Central for supplementary material.

Acknowledgments

We thank our patients and their families for generous support. We thank M.B. Lambros for technical support. This work was supported by a Prostate Cancer UK project grant (PG13–036 to JDB), a Movember/PCUK Programme grant to the London PCa Centre of Excellence, a Cancer Research UK Centre grant, a Prostate Cancer Foundation Global Challenge Award (to C.E. Barbieri, M.A. Rubin, J.S. de Bono) and a Royal Marsden Biomedical Research Centre flagship grant (A34 to J.S. de Bono). G. Boysen was supported by Marie Sklodowska-Curie Individual Fellowship. J. Mateo was supported by a Prostate Cancer Foundation Young Investigator Award.

References

1. Grasso CS, Wu YM, Robinson DR, Cao X, Dhanasekaran SM, Khan AP, et al. The mutational landscape of lethal castration-resistant prostate cancer. Nature 2012;487:239–43. [PubMed: 22722839]
2. Barbieri CE, Baca SC, Lawrence MS, Demichelis F, Blattner M, Theurillat J-P, et al. Exome sequencing identifies recurrent SPOP, FOXA1 and MED12 mutations in prostate cancer. Nat Genet 2012;44:685–9. [PubMed: 22610119]
3. Baca SC, Prandi D, Lawrence MS, Mosquera JM, Romanel A, Drier Y, et al. Punctuated evolution of prostate cancer genomes. Cell 2013;153: 666–77. [PubMed: 23622249]
4. The Cancer Genome Atlas Research Network. The molecular taxonomy of primary prostate cancer. Cell 2015;163:1011–25. [PubMed: 26544944]
5. Robinson D, Van Allen EM, Wu YM, Schultz N, Lonigro RJ, Mosquera JM, et al. Integrative clinical genomics of advanced prostate cancer. Cell 2015;161:1215–28. [PubMed: 26000489]
6. Blattner M, Lee DJ, O'Reilly C, Park K, MacDonald TY, Khani F, et al. SPOP mutations in prostate cancer across demographically diverse patient cohorts. Neoplasia 2014;16:14–20. [PubMed: 24563616]
7. Shenoy TR, Boysen G, Wang MY, Xu QZ, Guo W, Koh FM, et al. CHD1 loss sensitizes prostate cancer to DNA damaging therapy by promoting error-prone double-strand break repair. Ann Oncol 2017;28: 1495–507. [PubMed: 28383660]
8. An J, Wang C, Deng Y, Yu L, Huang H. Destruction of full-length androgen receptor by wild-type SPOP, but not prostate-cancer-associated mutants. Cell Rep 2014;6:657–69. [PubMed: 24508459]
9. Geng C, He B, Xu L, Barbieri CE, Eedunuri VK, Chew SA, et al. Prostate cancer-associated mutations in speckle-type POZ protein (SPOP) regulate steroid receptor coactivator 3 protein turnover. Proc Natl Acad Sci U S A 2013;110:6997–7002. [PubMed: 23559371]
10. Groner AC, Cato L, de Tribolet-Hardy J, Bernasocchi T, Janouskova H, Melchers D, et al. TRIM24 is an oncogenic transcriptional activator in prostate cancer. Cancer Cell 2016;29:846–58. [PubMed: 27238081]
11. Boysen G, Barbieri CE, Prandi D, Blattner M, Chae SS, Dahija A, et al. SPOP mutation leads to genomic instability in prostate cancer. Elife 2015;4: pii:e09207. [PubMed: 26374986]
12. Blattner M, Liu D, Robinson BD, Huang D, Poliakov A, Gao D, et al. SPOP mutation drives prostate tumorigenesis in vivo through coordinate regulation of PI3K/mTOR and AR signaling. Cancer Cell 2017;31:436–51. [PubMed: 28292441]
13. Dai X, Gan W, Li X, Wang S, Zhang W, Huang L, et al. Prostate cancer-associated SPOP mutations confer resistance to BET inhibitors through stabilization of BRD4. Nat Med 2017;23:1063–71. [PubMed: 28805820]
14. Zhang P, Wang D, Zhao Y, Ren S, Gao K, Ye Z, et al. Intrinsic BET inhibitor resistance in SPOP-mutated prostate cancer is mediated by BET protein stabilization and AKT-mTORC1 activation. Nat Med 2017; 23:1055–62. [PubMed: 28805822]
15. Lee D, Fontugne J, Gumpeni N, Park K, MacDonald TY, Robinson BD, et al. Molecular alterations in prostate cancer and association with MRI features. Prostate Cancer Prostatic Dis 2017;20:430–5. [PubMed: 28762374]
16. Attard G, Reid AH, A'Hern R, Parker C, Oommen NB, Folkerd E, et al. Selective inhibition of CYP17 with abiraterone acetate is highly active in the treatment of castration-resistant prostate cancer. J Clin Oncol 2009; 27:3742–8. [PubMed: 19470933]

17. Eisenhauer EA, Therasse P, Bogaerts J, Schwartz LH, Sargent D, Ford R, et al. New response evaluation criteria in solid tumours: revised RECIST guideline (version 1.1). Eur J Cancer 2009;45:228–47. [PubMed: 19097774]
18. Ferraldeschi R, Nava Rodrigues D, Riisnaes R, Miranda S, Figueiredo I, Rescigno P, et al. PTEN protein loss and clinical outcome from castration-resistant prostate cancer treated with abiraterone acetate. Eur Urol 2015;67:795–802. [PubMed: 25454616]
19. Rodrigues DN, Hazell S, Miranda S, Crespo M, Fisher C, de Bono JS, et al. Sarcomatoid carcinoma of the prostate: ERG fluorescence in-situ hybridization confirms epithelial origin. Histopathology 2015;66:898–901. [PubMed: 25041380]
20. Mateo J, Carreira S, Sandhu S, Miranda S, Mossop H, Perez-Lopez R, et al. DNA-repair defects and olaparib in metastatic prostate cancer. N Engl J Med 2015;373:1697–708. [PubMed: 26510020]
21. Seed G, Yuan W, Mateo J, Carreira S, Bertan C, Lambros M, et al. Gene copy number estimation from targeted next-generation sequencing of prostate cancer biopsies: analytic validation and clinical qualification. Clin Cancer Res 2017;23:6070–7. [PubMed: 28751446]
22. Garofalo A, Sholl L, Reardon B, Taylor-Weiner A, Amin-Mansour A, Miao D, et al. The impact of tumor profiling approaches and genomic data strategies for cancer precision medicine. Genome Med 2016; 8:79. [PubMed: 27460824]
23. DePristo MA, Banks E, Poplin R, Garimella KV, Maguire JR, Hartl C, et al. A framework for variation discovery and genotyping using next-generation DNA sequencing data. Nat Genet 2011;43:491–8. [PubMed: 21478889]
24. Ramos AH, Lichtenstein L, Gupta M, Lawrence MS, Pugh TJ, Saksena G, et al. Oncotator: cancer variant annotation tool. Hum Mutat 2015;36: E2423–9. [PubMed: 25703262]
25. Lek M, Karczewski KJ, Minikel EV, Samocha KE, Banks E, Fennell T, et al. Analysis of protein-coding genetic variation in 60,706 humans. Nature 2016;536:285–91. [PubMed: 27535533]
26. Genomes Project C, Auton A, Brooks LD, Durbin RM, Garrison EP, Kang HM, et al. A global reference for human genetic variation. Nature 2015;526:68–74. [PubMed: 26432245]
27. Sherry ST, Ward MH, Kholodov M, Baker J, Phan L, Smigielski EM, et al. dbSNP: the NCBI database of genetic variation. Nucleic Acids Res 2001;29:308–11. [PubMed: 11125122]
28. Forbes SA, Beare D, Boutselakis H, Bamford S, Bindal N, Tate J, et al. COSMIC: somatic cancer genetics at high-resolution. Nucleic Acids Res 2017;45:D777–83. [PubMed: 27899578]
29. Janouskova H, El Tekle G, Bellini E, Udeshi ND, Rinaldi A, Ulbricht A, et al. Opposing effects of cancer-type-specific SPOP mutants on BET protein degradation and sensitivity to BET inhibitors. Nat Med 2017; 23:1046–54. [PubMed: 28805821]

Translational Relevance

The genomic heterogeneity of prostate cancer has been elucidated, enabling the study of how genomic subclassification of these diseases associates with treatment outcome. These studies have identified *SPOP* mutations as early events in prostate tumorigenesis that commonly associate with *CHD1* loss and define a subclass of this disease. *SPOP* mutations have recently been reported to associate with increased androgen receptor (AR) signaling. We therefore hypothesized that prostate cancers with *SPOP* mutations would be highly sensitive to AR blockade and addressed this with regards to abiraterone treatment in efforts to develop predictive biomarkers of response to therapy. Abiraterone is a CYP17A1 inhibitor that improves survival from advanced prostate cancer. We found here that this subclass of prostate cancers has a very high sensitivity to AR signaling blockade with abiraterone, with most *SPOP*-mutated/*CHD1* -deleted cancers responding to this.

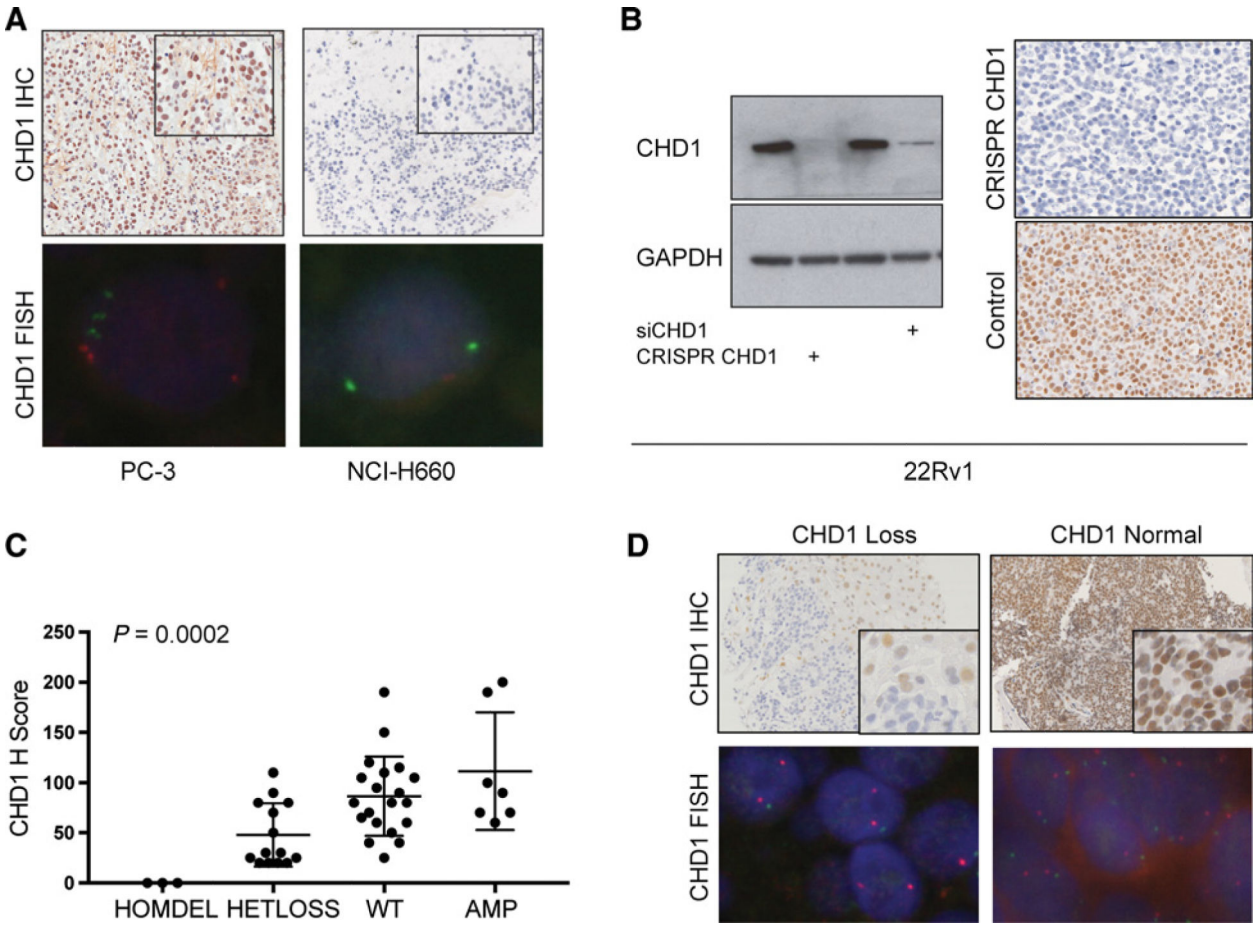

Figure 1.

Development and validation of CHD1 IHC assay. **A,** Micrographs (20×) of FFPE prostate cancer cells negative (NCI-H660) or positive for CHD1 analyzed by CHD1 IHC (top) and FISH (below). Signals from the FISH probes (CHD1: red; reference probe: green). **B,** Knockdown of CHD1 by siRNA or CRISPR/CAS9 decreases CHD1 protein levels in 22Rv1 cells by Western blotting (left) and IHC on FFPE cells using the same antibody as in **A**. **C,** Correlation of CHD1 copy number and expression level in 44 prostate cancer samples. Numbers for HSPC and CRPC are indicated. Protein expression was summarized as H-scores. $P = 0.002$, one-way ANOVA. **D,** Micrographs of representative examples of CHD1 loss and CHD1 normal by IHC (20×) and FISH (60×). Signals from the FISH probes (CHD1: green; reference probe: red).

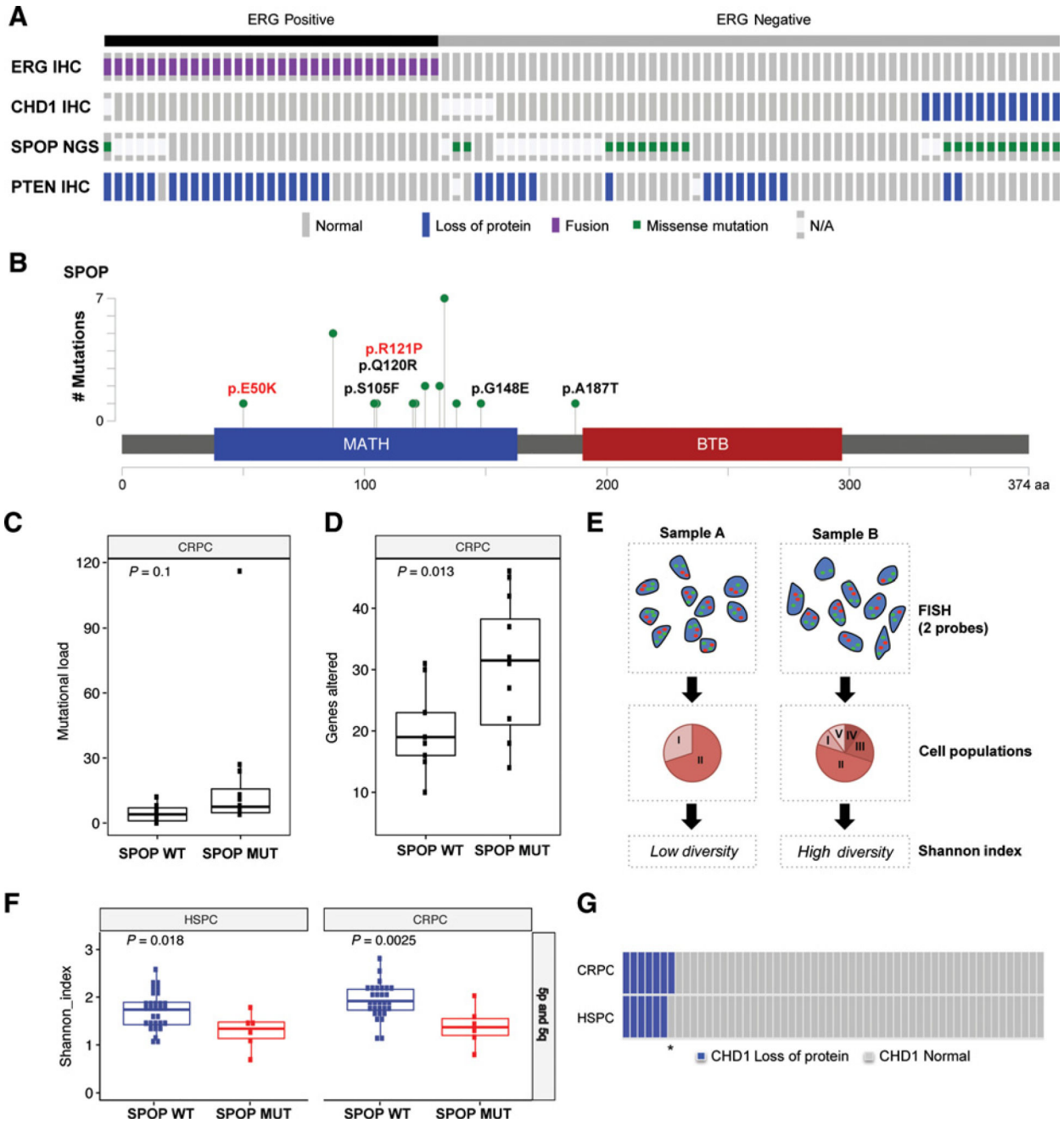

Figure 2.

Molecular characterization of the CRPC cohort. **A,** Oncoprint summarizing CHD1, ERG, and PTEN protein expression, as well as *SPOP* mutation status in mCRPC biopsies from 89 patients. **B,** Lollipop blot representing the location of the affected amino acid changes in the SPOP protein corresponding to the 22 identified mutations. **C** and **D,** Genomic features of *SPOP* mutant CRPC estimated by a targeted NGS assay ($n = 46$). The levels of mutational burden do not change in *SPOP*-mutant CRPC ($P = 0.1$; **C**). Copy-number burden estimated by the percentages of genes affected are significantly higher in *SPOP*-mutant CRPC compared with *SPOP* wild-type disease ($P = 0.013$; **D**). *P* values were calculated using

unpaired *t* test. **E,** Workflow describing how the Shannon index was calculated. We counted the signals from a dual FISH assay containing probes for 5p and 5q on a single-cell level for each patient. FISH probes are indicated by red and green dots in the cell nucleus (blue). Different cell populations are then defined by possible probe combination reflecting the diversity of copy-number differences at these genomic loci per tumor cell. The frequency of these different cell populations in a given biopsy reflects population diversity, which is estimated using the Shannon index. **F,** *SPOP*-mutant tumors have a significantly lower mean Shannon index than *SPOP* wild-type tumors in both HSPC and CRPC biopsies (HSPC: $P = 0.018$, CRPC: $P = 0.0025$). Mean Shannon indices for each subclass do not change from HSPC to CRPC. *P* values were calculated using unpaired *t* test. $n = 36$. **G,** CHD1 protein level in HSPC and CRPC biopsies. Heatmap summarizing CHD1 expression status (loss vs. normal) in 56 patient-matched paired biopsies from HSPC and CRPC. Blue, protein loss; gray, protein expression.

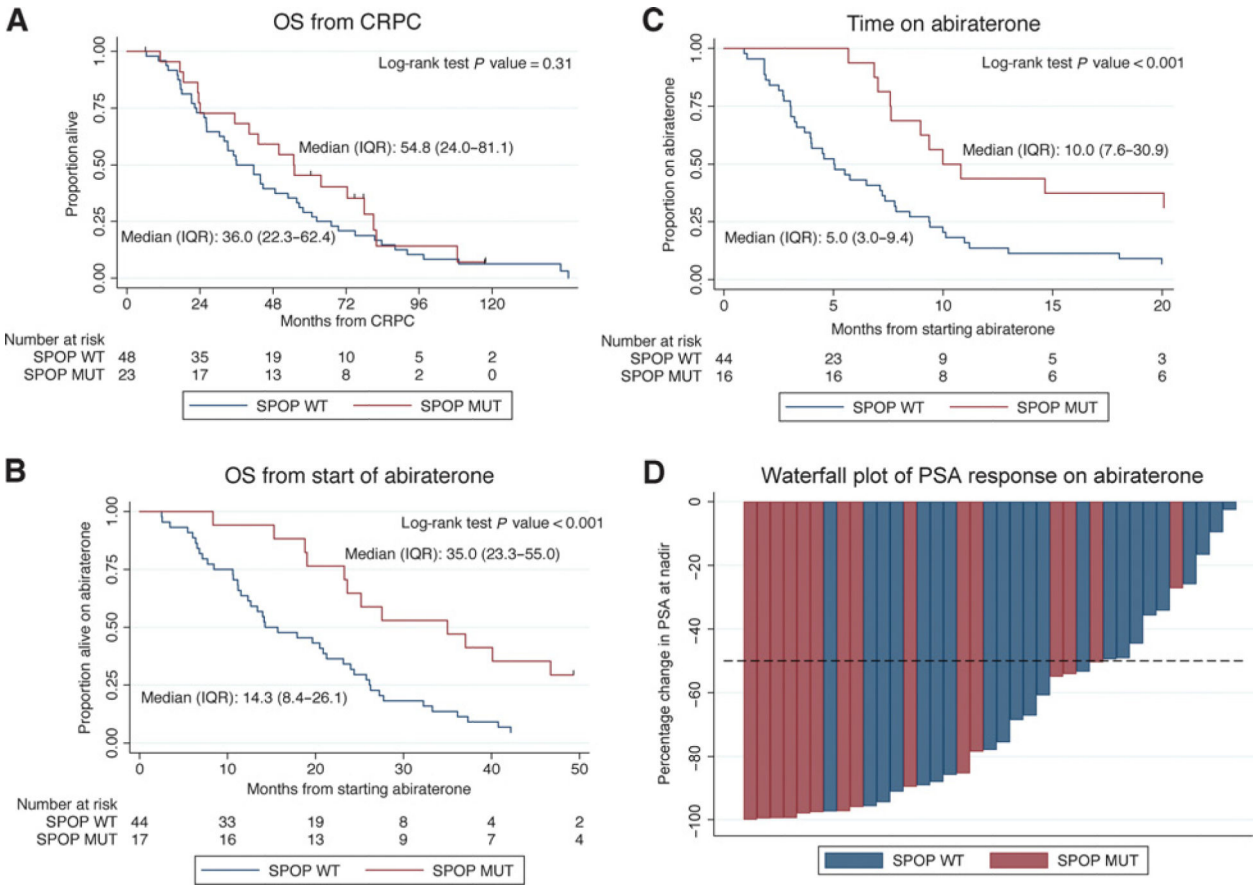

Figure 3.

Association of CHD1 loss and *SPOP* mutation with clinical outcome. **A,** Kaplan-Meier curve summarizing OS of $SPOP^{MUT}$ versus $SPOP^{WT}$ tumors from CRPC in this cohort. *SPOP* mutation is not prognostic. **B** and **C,** Kaplan-Meier curves showing increased survival from start of abiraterone (**B**) and time on abiraterone (**C**) in *SPOP*-mutant tumors. **D,** Waterfall plot showing increased PSA responses from start of abiraterone in $SPOP^{MUT}$ versus $SPOP^{WT}$ tumors. Each bar represents PSA nadir from the start of the treatment for an individual patient. Dashed line indicates PSA fall by 50%. PSA nadir data were available for 37 patients with known SPOP status.

Table 1.

Demographic and clinical characteristics of patients in this cohort

Overall (*n* = 89) **Lacking CHD1 IHC *n* = 6 (6.7%)**	**CHD1 negative in CRPC *n* = 13 (14.6%)**	**CHD1 positive in CRPC *n* = 70 (78.7%)**	***P***
Age at diagnosis, years (mean, SD)	62.7 (6.8)	59.9 (13.1)	$P = 0.46^a$
Gleason at diagnosis			
6	2 (15%)	5 (7%)	$P = 0.71^b$
7	2 (15%)	16 (23%)	
8–10	8 (62%)	44 (63%)	
NA	1 (8%)	5 (7%)	
Metastasis at diagnosis			
M0	5 (39%)	43 (61%)	$P = 0.14^b$
M1	8 (62%)	27 (39%)	
PSA at diagnosis, ln (μg/L; mean, SD)	4.8 (1.6)	5 (1.6)	$P = 0.82^a$
Treatments for CRPC			
Docetaxel	11 (85%)	64 (93%)	$P = 0.31^b$
Abiraterone	9 (69%)	62 (90%)	$P = 0.07^b$

[a] *t* test.

[b] Fisher exact test.

Table 2.

Summary of univariate statistical analyses evaluating the association of CHD1 loss or *SPOP* mutation with response to LHRHa and abiraterone

	Univariate HR	**95% CI**	***P***
Overall survival from diagnosis			
Metastatic at diagnosis	2.07	1.32–3.24	0.002
SPOP mutation at CRPC	0.80	0.46–1.38	0.43
CHD1 negative IHC at CRPC	0.81	0.42–1.58	0.54
ERG at CRPC	1.14	0.72–1.78	0.58
Time on abiraterone	**Univariate HR**	**95% CI**	***P***
Metastatic at diagnosis	1.00	0.63–1.60	0.99
SPOP mutation at CRPC	0.37	0.20–0.69	0.002
CHD1 negative IHC at CRPC	0.50	0.25–1.02	0.06
ERG at CRPC	1.25	0.77–2.02	0.37
Time from start LHRH to CRPC	**Univariate HR**	**95% CI**	***P***
Metastatic at diagnosis	2.11	1.36–3.28	0.001
SPOP mutation at CRPC	1.13	0.68–1.87	0.64
CHD1 negative IHC at CRPC	0.86	0.44–1.69	0.66
ERG at CRPC	1.16	0.75–1.79	0.52
Response to abiraterone	**Univariate OR**	**95% CI**	***P***
Metastatic at diagnosis	0.72	0.29–1.80	0.49
SPOP mutation at CRPC	14.50	2.92–71.94	0.001
CHD1 negative IHC at CRPC	7.30	0.82–65.11	0.08
ERG at CRPC	0.71	0.28–1.82	0.47